*Journal of Engineering*

WILEY

RESEARCH ARTICLE OPEN ACCESS

# Mechanical Performance of Black Cotton Soil Stabilised With Bagasse Ash Incorporating Limestone Calcined Clay Cement Under Varied Loading Conditions

Horris K. Nangulama[1,2] | Siya P. Rimoy[1] | John Elvis[1]

[1]Department of Transportation and Geotechnical Engineering, College of Engineering and Technology, University of Dar es Salaam, Dar es Salaam, Tanzania | [2]Department of Mining Engineering, School of Engineering, Malawi University of Business and Applied Sciences, Blantyre, Malawi

**Correspondence:** Horris K. Nangulama (hnangulama@mubas.ac.mw)

**Received:** 10 February 2026 | **Revised:** 28 July 2026 | **Accepted:** 5 August 2026

**Academic Editor:** Shikha Binwal

**Keywords:** bagasse ash | black cotton soil | lc3 cement | soil stabilisation | sustainable materials

## ABSTRACT

Construction of geotechnical infrastructures in tropical regions characterised by black cotton soil (BCS) presents major engineering challenges due to its high swelling and shrinkage potential. Bagasse ash (BA) incorporating limestone calcined clay cement ($LC^3$) has emerged as a promising stabilisation approach to enhance the performance of foundations constructed on BCS. In this study, BCS specimens were stabilised using a BA-$LC^3$ binder at proportions ranging from 0% to 18% by dry mass of soil and cured for 7–28 days at temperatures of 10°C and 32°C to evaluate their mechanical response under loading conditions. Consolidated drained direct shear and triaxial tests were conducted under varying confining pressures to assess the mechanical performance of the treated BCS. The results show that the peak shear strength of treated BCS increased with increasing confining pressure, curing period and curing temperature. Shear strength increased by 76.2% on average, considering 450-kPa confining pressure, 28-day curing period and 32°C curing temperature. An optimal BA-$LC^3$ binder content for BCS was found to obtain the highest internal friction angle, which ranged around 15% content at 28 curing days and 32°C curing temperature. Failure behaviour also varied significantly between untreated and treated soils. Untreated BCS exhibited ductile behaviour, whereas BA-$LC^3$ stabilised BCS presented brittle behaviour. The findings demonstrate the feasibility of using BA-$LC^3$ binder system to improve the shear behaviour of BCS for geotechnical applications in tropical regions. This approach supports sustainable construction practices by reducing cement consumption, lowering carbon emissions and decreasing infrastructure development costs.

## 1 | Introduction

The rapid accumulation of greenhouse gases, particularly carbon dioxide ($CO_2$), has intensified global climate warming and poses serious environmental threats worldwide [1, 2]. The cement industry alone is responsible for about 9.1% of global $CO_2$ emissions annually [2–4]. Within the broader construction sector, infrastructure development accounts for nearly 40% of energy-related carbon emissions [3]. These emissions are projected to increase by 10-15% in the near future due to rapid urbanisation and industrialisation [3–6], which have led to significant growth in geotechnical infrastructure such as roads, buildings and foundations [5–7]. At the centre of this issue is ordinary Portland cement (OPC), which remains the most widely used construction material due to its reliable strength and durability properties [2–6]. However, OPC production is associated with a substantial carbon footprint [1–3]. Approximately 1000 kg of $CO_2$ is emitted during the production of 1.0 t of OPC [2, 4, 8]. This high emission level results primarily from the energy-intensive manufacturing process, which requires temperatures ranging between 1400°C and 1600°C, leading to significant anthropogenic $CO_2$ emissions [3–6]. According to Izumi et al.

[1] and Ijaz et al. [3], OPC production contributes approximately 4.8% of global $CO_2$ emissions, alongside other pollutants such as nitrogen oxides, sulphur oxides and dust. The extensive use of OPC in construction activities, including black cotton soil (BCS) stabilisation, has therefore raised significant environmental concerns [9–12]. In addition, when large-scale BCS stabilisation is required, the consumption of OPC becomes both economically expensive and environmentally unsustainable [10, 11]. Consequently, there has been a growing global interest in developing sustainable and cost-effective construction materials over the past decades to reduce dependence on OPC [4–6].

Researchers worldwide are actively investigating silica-rich industrial by-products as alternative materials to reduce the consumption of OPC in construction [13–18]. Several studies have explored the use of geopolymer-based industrial by-products, including ground granulated blast furnace slag (GGBS), fly ash and silica fume [8, 13, 19]. These materials, commonly referred to as supplementary cementitious materials (SCMs), have the potential to significantly reduce the carbon footprint of cement-based construction [12–15]. In addition to their environmental benefits, SCMs often exhibit high pozzolanic reactivity, which can improve the mechanical and durability properties of cementitious composites [2, 5]. For example, fly ash and GGBS are widely incorporated into concrete mixtures as partial replacement of OPC [13, 15]. This practice has been shown to enhance both mechanical performance and durability while simultaneously providing environmental and economic benefits [15, 20]. These materials have also been applied to stabilise problematic soils such as BCS [21, 22]. Studies indicate that incorporating fly ash or GGBS can significantly improve the engineering properties of treated BCS in a more sustainable and cost-effective manner [21–23]. However, when the OPC replacement ratio exceeds certain limits, the performance of fly ash or GGBS-based systems may deteriorate [10, 20]. Furthermore, in countries such as Malawi, where electricity generation relies less on fossil fuels, the availability and quality of fly ash and GGBS are limited. This restricts their large-scale use in cement production and soil stabilisation. In addition, the practical implementation of geopolymer-based materials is still largely considered a medium- to long-term solution due to limitations related to accessibility, reactivity and variability in soil performance [21–23].

Bagasse ash (BA) has demonstrated considerable potential as a partial replacement material for OPC in both concrete production and soil stabilisation applications [24–29]. However, the disposal of BA remains a significant environmental challenge in sugar-producing regions such as Shire Valley in Malawi [26]. Bagasse, the fibrous residue obtained after extracting juice from sugarcane, is commonly burned as fuel for electricity generation in sugar processing industries, producing BA as a waste by-product [25]. Approximately 30-45 kg of BA can be produced from 1.0 t of bagasse waste [8]. BA generated from boiler cleaning processes in sugar mills, such as ILLOVO Sugar Company Ltd., often exhibits relatively low loss on ignition (LOI) and contains high concentrations of silica ($SiO_2$) and alumina ($Al_2O_3$), which are key indicators of pozzolanic activity [26, 29, 30]. Several studies have demonstrated the potential use of BA in cementitious materials. For example, Wu et al. [24] replaced OPC with BA in the range of 0%–30% during concrete production and found that mixtures containing 25% BA exhibited satisfactory workability and strength properties. Similarly, Serker et al. [27] reported that 30% BA replacement produced optimum compressive strength in modified concrete mixtures. Chindaprasirt et al. [28] observed that replacing 60% of OPC with BA reduced $CO_2$ emissions by 57% and energy consumption by 55% compared with conventional OPC mortars. However, despite its promising characteristics, the use of BA alone may not be sufficient to meet the strength and serviceability requirements for stabilising BCS in geotechnical construction [25]. Previous studies have shown that when BA is used as the sole stabilising material, vertical displacement and deformation may increase in treated BCS [9, 30]. To address this limitation, researchers have explored the incorporation of additional materials such as lime, fly ash, dolomite and synthetic fibres together with BA [29–32]. These studies reported reductions in the plasticity of treated BCS, although improvements in California bearing ratio were often limited. The incorporation of BA with OPC has been found to significantly enhance the unconfined compressive strength of treated BCS while simultaneously reducing BA waste disposal challenges [25, 29, 30]. Moreover, BA-OPC stabilised BCS has shown reductions in free swell potential and optimum moisture content, accompanied by increases in maximum dry density and shear strength [33, 34]. However, the utilisation of OPC as an incorporating material to BA might raise the carbon footprint environmental concerns and seriously increase the BCS stabilisation cost as compared with the related benefits [1–6].

Limestone calcined clay (CC) cement ($LC^3$) is an emerging low-carbon cementitious material capable of reducing $CO_2$ emissions by up to 40% compared with OPC [3, 35, 36]. $LC^3$ typically consists of limestone, CC and clinker, with its mechanical performance largely depending on the proportions of these components [36–38]. The synergistic effect between CC and limestone contributes to enhanced hydration reactions and improved mechanical properties of $LC^3$-based composites [35]. Moreover, $LC^3$ manufacture does not require new technologies, making it inexpensive and easy to introduce to the geotechnical construction sector [37]. Compared with OPC, the notable features of $LC^3$ lie in being able to reduce the consumption of ground clinker by about 50% while facilitating the dense rheological formation just as OPC, leading to enhanced mechanical strength and improved durability [39–41]. Several studies have evaluated the performance of $LC^3$ in construction materials. For instance, Mohamed et al. [39] investigated the effect of CC on $LC^3$ concrete, whereas Sharma et al. [40] examined its hydration behaviour. Some recent studies by Wang et al. [42] and Reddy et al. [43], respectively, centred on stabilisation of zinc and radioactive-borate-contaminated soils with $LC^3$ and demonstrated its capacity to alter the properties of treated soils through hydration reaction. Field studies conducted in Kenya and India demonstrated that $LC^3$ can reduce carbon emissions by approximately 40% when used in soil stabilisation and concrete pavements compared with OPC [44, 45]. Just as Ijaz et al. [3], Scrivener et al. [36] showed that $LC^3$ can be applied in the same way as OPC and does not need a special training. Thus, BA can be incorporated with $LC^3$ in the same manner as BA is incorporated with OPC [46, 47]. Overall, a combined use of BA and $LC^3$ as cementitious material has a significant potential to meet the extensive amounts of materials demanded by the cement industry for routine BCS stabilisation practice to ensure more green, cost-effective, sustainable and resilient geotechnical constructions.

Although both BA and $LC^3$ have individually demonstrated promising potential in soil stabilisation, studies investigating their combined application for stabilising BCSs remain limited. In particular, the behaviour of BA-$LC^3$ stabilised BCS under varying pressure and curing conditions has not been adequately investigated. Despite that many engineering challenges arise at low pressures, investigating the behaviour of soil at high pressures is crucial to fathom better engineering construction conditions [48–50]. In addition, Nguyen et al. [51] observed that the cementation effects of treated soils were notably apparent under low confining pressures, with shear strength arising from the precipitated surface roughness. These studies have uncovered that shear strength intensifies with an increase in pressure and curing conditions, as showcased by Malandraki et al. [52] and Sariosseiri et al. [53]. Hence, this study purposes to evaluate the shear strength and mechanical behaviour of treated BCS through consolidated drained (CD) direct shear and triaxial tests under high pressures ranging from 50 to 1000 kPa considering different curing conditions. These pressures tally with different depths of foundations for roads and buildings.

Therefore, this study delves into the mechanical properties and BA-$LC^3$ binder content of treated BCS under varied loading and curing while evaluating the correlation between influencing factors and the resulting strength improvement. Direct shear strength was performed to analyse the effect of mechanical characteristics on binder content, vertical pressure, curing age and curing temperature for treated BCSs. Different test sets were conducted under triaxial tests to analyse the maximum deviatoric stress, maximum volumetric strain, stress ratio, postyield strain-softening and postyield strain-hardening behaviour of the treated BCS subjected to high confining pressures. Subsequently, an attempt was made to rank the factors influencing the shear behaviour of BA-$LC^3$ binder-treated BCS using a grey relational analysis, which can help to provide insights into foundation design on BCSs. The findings from this study are expected to contribute to the development of sustainable, cost-effective and environmentally friendly BCS stabilisation techniques suitable for geotechnical construction in tropical regions.

## 2 | Materials and Methods

BA, $LC^3$, and BCS were the primary materials used in this study. All materials were collected from the Shire Valley region in Malawi, which lies at elevations ranging from 34-106 m above sea level, between 34°15′E–35°16′E longitude and 15°29′S–16°46′S latitude, leading to tropical conditions in the area.

BA was obtained from ILLOVO Sugar Company Ltd during the boiler cleaning process. The ash was collected from boilers operating at approximately 600°C, consistent with procedures reported in previous studies [9, 28]. This temperature is considered optimal for removing residual carbon while preserving amorphous silica, which enhances the pozzolanic reactivity of BA [30]. After collection, the ash was allowed to cool to room temperature, manually ground into powder form, and sieved through a 300-$\mu$m sieve to remove impurities and coarse particles [24]. The measured physical properties of BA indicated a specific gravity of 2.52, a median particle size ($d_{50}$) of 26.97 $\mu$m, and a Blaine surface area of 513 $m^2$/kg. The material was observed to be black in colour. To determine its pozzolanic characteristics, the chemical composition of BA was analysed using a Xenemetrix X-Calibur X-ray fluorescence (XRF) spectrometer, and the results are presented in Table 1. According to ASTM C618 [58], a natural pozzolana containing a combined

**TABLE 1** | Engineering properties of BA, $LC^3$ and BCS materials.

| Chemical properties | $SiO_2$ (%) | $Al_2O_3$ (%) | $Fe_2O_3$ (%) | CaO (%) | $Na_2O$ (%) | $SO_3$ (%) | MgO (%) | $K_2O$ (%) | LOI (%) |
|---|---|---|---|---|---|---|---|---|---|
| BA | 59.37 | 6.66 | 6.41 | 15.89 | 1.07 | 1.79 | 3.14 | 3.31 | 2.11 |
| $LC^3$ | 26.43 | 5.01 | 3.36 | 58.37 | 0.14 | 3.13 | 1.51 | 0.46 | 1.57 |
| BCS | 65.63 | 10.25 | 7.03 | 0.59 | 2.18 | 1.84 | 4.16 | 1.35 | 6.93 |
| **Physical properties of BCS** | | | | | | **Test method** | | **Mean value** | |
| Natural moisture content | | | | | | ASTM D2216 [54] | | 36.7% | |
| Specific gravity | | | | | | ASTM D854 [55] | | 2.3 | |
| Plasticity | | | | | | ASTM D4318 [56] | | — | |
| Liquid limit | | | | | | — | | 80.3% | |
| Plastic limit | | | | | | — | | 33.2% | |
| Plasticity index | | | | | | — | | 47.1% | |
| Particle size distribution | | | | | | ASTM D6913 [57] | | — | |
| Clay | | | | | | — | | 62.5% | |
| Silt | | | | | | — | | 27.8% | |
| Sand | | | | | | — | | 9.7% | |
| Gravel | | | | | | — | | 0.0% | |

Abbreviations: $Al_2O_3$ = aluminium oxide; $Fe_2O_3$ = iron oxide; CaO = calcium oxide; $K_2O$ = potassium oxide; LOI = loss on ignition; MgO = magnesium oxide; $Na_2O$ = sodium oxide; $SiO_2$ = silicon oxide; $SO_3$ = sulphur trioxide.

percentage of $SiO_2$, $Al_2O_3$ and $Fe_2O_3$ greater than 70% is classified as a Class F pozzolanic material. Based on this criterion, the analysed BA qualifies as Class F pozzolana.

To prepare $LC^3$, locally sourced kaolinite clay was first calcined in a furnace at 800°C ± 10°C for 30 min to produce CC. This temperature corresponds to the dehydroxylation range of kaolinite clay minerals, which promotes the formation of highly reactive metakaolin [37]. The selected calcination duration of 30 min represents the minimum period required to ensure complete structural transformation of kaolinite [37]. Limestone (LS) and gypsum (Gyp) were separately ground into fine powder. Clinker (CL) was obtained from the Shayona Portland Cement Manufacturing (SPCM) distributor. Only materials passing through a 75 $\mu$m sieve were used in the preparation of $LC^3$ to ensure uniform particle size. The $LC^3$ was prepared according to the typical composition reported in previous studies, consisting of 30% CC, 15% limestone, 5% gypsum, and 50% clinker [36–40]. The mineralogical composition of the prepared $LC^3$ was determined using XRF analysis, and the results are presented in Table 1.

**TABLE 2** | Compaction parameters of untreated and treated BCS specimens.

| BA-$LC^3$ binder content (%) | MDD ($kN/m^3$) | OMC (%) |
|---|---|---|
| 0 | 16.30 | 19.1 |
| 3 | 16.31 | 19.0 |
| 6 | 16.37 | 18.8 |
| 9 | 16.38 | 18.7 |
| 12 | 16.43 | 18.3 |
| 15 | 16.49 | 17.9 |
| 18 | 16.55 | 17.6 |

BCS samples were collected from a depth of 1.5 m below ground surface to minimise contamination from organic matter and surface debris [11, 26]. The collected soil was oven-dried at 105°C for 24 hours to remove moisture [25]. The dried soil was then sieved through a 2.0 mm sieve to remove coarse particles and obtain uniform specimens for testing [21]. The engineering properties of the soil were subsequently determined, and the results are summarised in Table 1. These values fall within the typical ranges reported for BCS in previous studies [11, 21, 26]. Based on the obtained properties, the soil was classified as fat clay (CH) as per the unified soil classification system. This classification

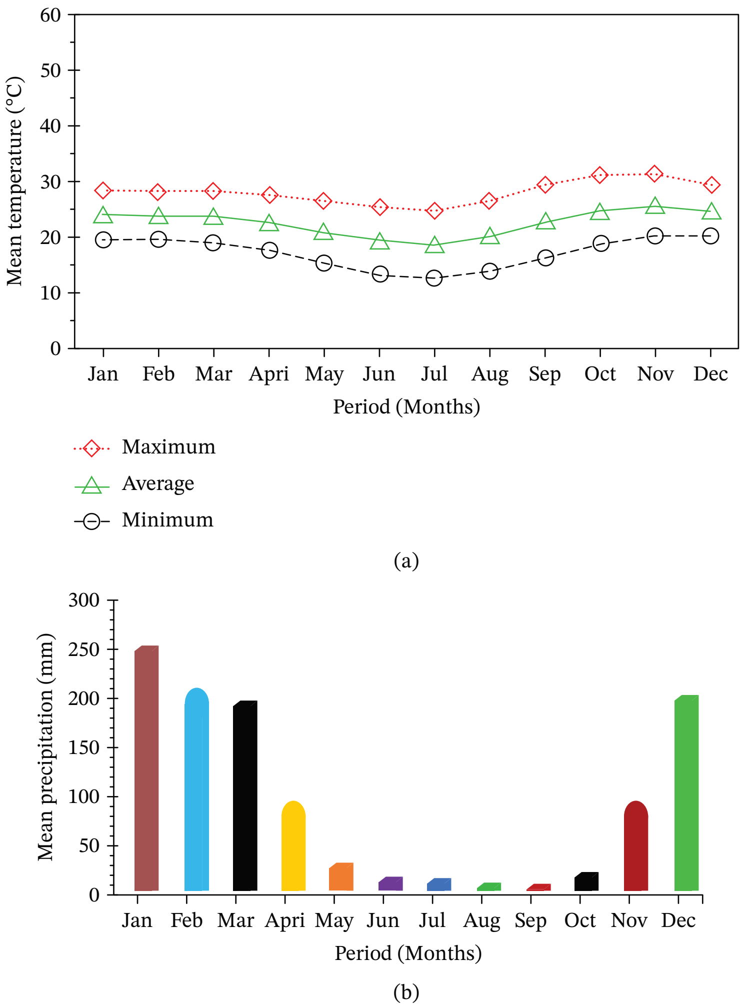


**FIGURE 1** | Tropical climatic conditions of Shire Valley from 1991 to 2025 [60]: (a) temperature per month and (b) precipitation per month.

indicates that the soil exhibits high plasticity and swelling potential, making it unsuitable for direct use as a foundation material in geotechnical construction without stabilisation [9–12].

BA was incorporated with $LC^3$ at a mass ratio of 3:2, consistent with proportions reported in previous studies [26]. The BA-$LC^3$ binder mixture was added to BCS at contents ranging from 0% to 18% by dry weight of soil to evaluate its influence on the shear strength behaviour of stabilised soil. The BCS specimens were compacted using a standard compaction energy of 600 kN-m/$m^3$, corresponding to 95% of the maximum dry density (MDD). To compensate for potential moisture loss during mixing and curing and to facilitate hydration reactions, the moisture content was adjusted to 2.5% above the optimum moisture content (OMC). This approach is consistent with practices adopted in field stabilisation of expansive soils [32]. Standard Proctor compaction tests were conducted in accordance with ASTM D698 [59]. The resulting MDD and OMC values for untreated and treated specimens are tabulated in Table 2.

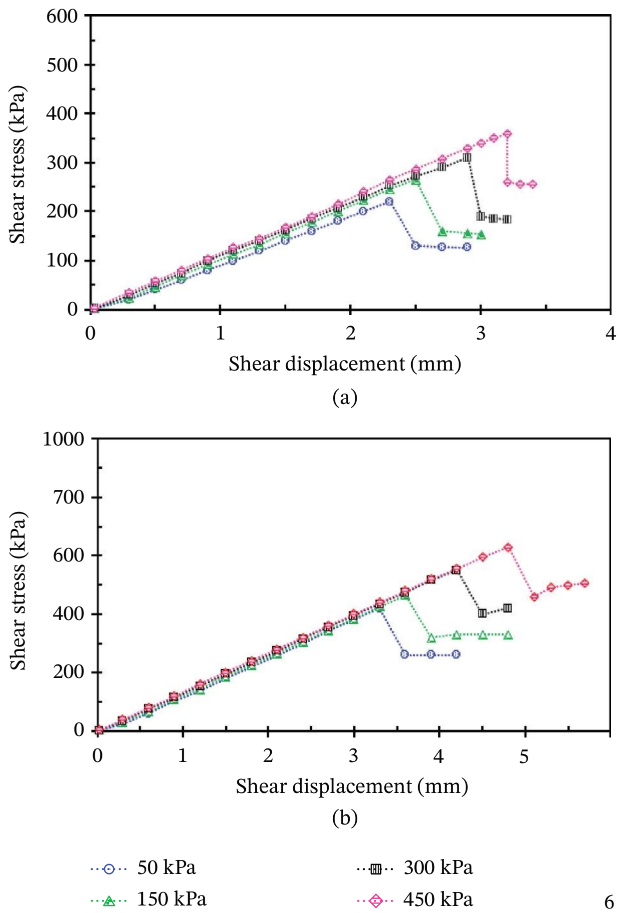


**FIGURE 2** | Shear–stress displacement relationship of treated BCS: (a) at +10°C curing temperature and (b) at +32°C curing temperature.

Direct shear tests were conducted inside a temperature-controlled chamber where the temperature ranged between 10°C and 32°C (±0.1°C accuracy) to simulate the climatic conditions of the Shire Valley region in Malawi. The minimum and maximum testing temperatures were selected based on long-term mean temperature records of the study area, as portrayed in Figure 1. Specimens were cured at 7, 14, and 28 days and tested under vertical normal stresses of 50, 150, 300, and 450 kPa. Direct shear tests were performed following the procedures specified in ASTM D3080 [61], using specimens compacted at MDD and OMC conditions. After compaction, specimens were sealed with plastic films to prevent moisture loss and cured at standard 95% relative humidity and 24°C temperature. The shear tests were conducted at a constant displacement rate of 2.4 mm/min, and shear stress was calculated using the following equation:

$$\tau = \frac{GC}{A}, \qquad (1)$$

where

$\tau$ = shear stress of the specimen;

$A$ = sheared area of the specimen;

$G$ = loop gauge reading;

$C$ = loop calibration constant.

In addition to direct shear testing, triaxial CD compression tests were performed on untreated BCS and BCS stabilised with 15% BA-$LC^3$ binder, which corresponded to the optimum binder content identified in preliminary tests. The specimens were cured for 28 days and subjected to confining pressures of 50, 150, 300, 450, 600, 750, 900, and 1000 kPa to evaluate the behaviour of the treated soil under a wider range of stress conditions. After compaction, specimens were subjected to vacuum saturation followed by curing in water at a standard 24°C temperature. Compared with direct shear tests, the triaxial shear tests were performed at a standard 24°C temperature to prevent thermal variations from affecting the pore water pressure in the triaxial system [52]. Vacuum saturation was applied to minimise matric suction effects, ensuring that the measured strength reflected true effective stress conditions. The triaxial tests were conducted according to ASTM D7181 [62]. Before testing, drainage lines were flushed with de-aired water to eliminate trapped air within the triaxial system. The specimens were then mounted on a permeable base, and a top cap was installed. Filter paper

**TABLE 3** | Governing chemical reaction processes.

| Process | Chemical reaction | Compound |
|---|---|---|
| Hydration | $CaO + H_2O \rightarrow Ca(OH)_2$ | Calcium hydrate (CH) |
| Pozzolanic | $Ca(OH)_2 + SiO_2 \rightarrow 3CaO.2SiO_2.3H_2O$ | Calcium silicate hydrate (CSH) |
| Pozzolanic | $Ca(OH)_2 + Al_2O_3 \rightarrow 4CaO.Al_2O_3.13H_2O$ | Calcium alumina hydrate (CAH) |
| Dissolution | $Ca(OH)_2 \rightarrow Ca^{2+} + 2OH^-$ | Calcium and hydroxide ions |

discs were placed between the specimen ends and the porous stones to prevent migration of fine particles into the drainage system [63]. A constant strain rate of 0.2 mm/min was applied during testing to minimise potential creep effects, following procedures reported by Malandraki et al. [52].

## 3 | Results and Discussions

### 3.1 | Direct Shear Behaviour

For geotechnical structures founded on BCS in tropical regions, stability is a critical design requirement. Therefore, a comprehensive direct shear testing programme was conducted to evaluate the resistance of BA-LC$^3$ stabilised BCS under a wide range of static loading conditions. The mechanical improvement of treated BCS was evaluated using the shear–stress displacement (SSD) relationship, considering the effects of BA-LC$^3$ binder content, initial dry density, and curing conditions on the direct shear strength behaviour of the treated soil.

The SSD relationship of BA-LC$^3$ binder-treated BCS at curing temperatures of +10°C and +32°C is presented in Figure 2. During shearing, the specimens initially reached a peak shear strength, after which partial failure occurred. This behaviour resulted from the propagation of microcracks, which eventually led to failure of the entire specimen. The SSD curves of treated BCS exhibited distinct peaks at different BA-LC$^3$ binder contents. Furthermore, the peak shear strength increased with increasing vertical pressure. This behaviour can be attributed to the hydration reaction between the primary chemical compounds of the BA-LC$^3$ binder and water present in the soil matrix. Table 3 summarises the principal chemical reactions occurring within the BA-LC$^3$ binder-BCS system. The formation of hydration products such as calcium silicate hydrate (CSH) and calcium aluminosilicate hydrate (CASH) significantly contributed to the cementation of soil particles. This process improved the soil pore structure by reducing porosity and enhancing interparticle bonding, which ultimately resulted in increased shear strength. The failure patterns of untreated and treated BCS differed considerably. Untreated BCS exhibited ductile failure behaviour, whereas BA-LC$^3$ stabilised BCS displayed brittle failure characteristics due to reduced plasticity and enhanced particle bonding caused by hydration products.

Figures 3 and 4 illustrate the effect of BA-LC$^3$ binder content on the shear strength behaviour of treated BCS specimens. The results show that shear strength increased with increasing BA-LC$^3$ binder content. For instance, for specimens cured at +10°C at 28 days, the shear strengths of BCS treated with 18% BA-LC$^3$ binder under vertical pressures of 50, 150, 300, and 450 kPa were 360.32, 481.65, 559.33, and 640.01 kPa, respectively.

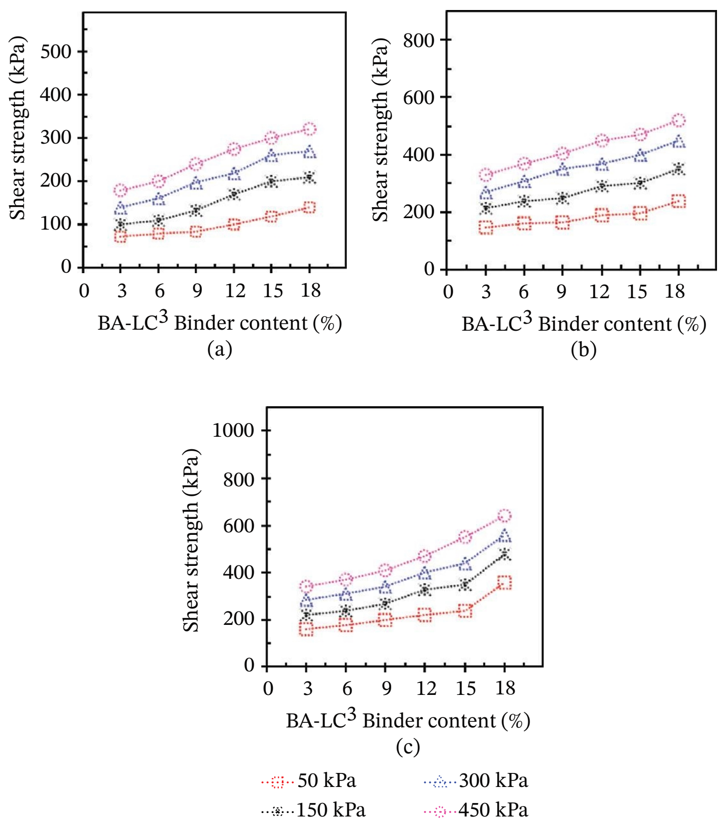


**FIGURE 3** | Effect of BA-LC$^3$ binder content on shear strength of treated BCS at +10°C curing temperature: (a) 7 curing days, (b) 14 curing days and (c) 28 curing days.

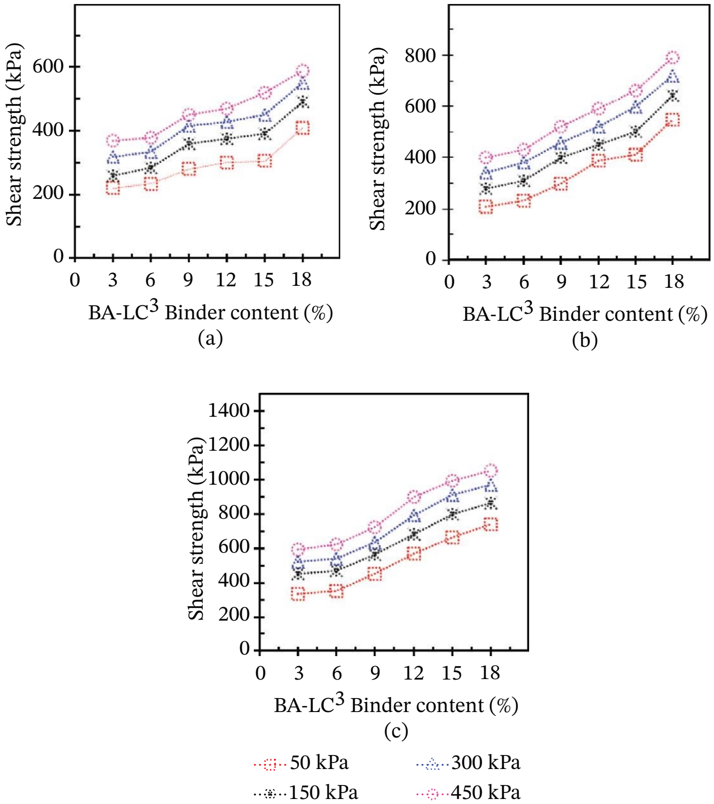


**FIGURE 4** | Effect of BA-LC³ binder content on shear strength of treated BCS at +32°C curing temperature: (a) 7 curing days, (b) 14 curing days and (c) 28 curing days.

Compared with specimens treated with 3% binder, the corresponding shear strength increased by 125%, 118.2%, 96.5%, and 88.2%, respectively. This improvement can be attributed to the increased formation of hydration products resulting from higher binder contents. These hydration products formed cementitious bonds at particle interfaces, which strengthened the soil skeleton and reduced pore spaces. Additionally, the improved shear strength can be explained by the microstructural modifications, whereby more cementitious compounds such as CASH gels were formed on treated BCS compared with untreated BCS (Figure 5). This phenomenon reduced interparticle spacing and decreased pore sizes. These changes enhanced the compactness, strength and structural integrity of the treated BCS.

Figures 3 and 4 also demonstrate that shear strength increased with increasing vertical pressure, curing period, and curing temperature. The highest shear strength values were consistently obtained for specimens treated with 18% BA-LC³ binder under a vertical pressure of 450 kPa. This behaviour can be attributed to the combined effects of particle breakage and cementation. Under relatively low vertical pressures, the treated BCS exhibited brittle behaviour and resisted shear primarily through bonding strength and particle interlocking. At higher vertical pressures, the shear resistance was mainly governed by particle strength, rearrangement, and fragmentation. This observation is consistent with the findings of Nagaraj and Miura [64], who reported that increasing vertical pressure leads to particle fragmentation and structural rearrangement, resulting in denser soil configurations. Similar observations have been reported by Kang et al. [65] and Pu et al. [66].

The shear strength of BA-LC³ binder-treated BCS cured at +10°C (Figure 3) was consistently lower than that of specimens cured at +32°C (Figure 4). For instance, at +32°C curing temperature, the maximum shear strengths of BCS treated with 18% BA-LC³ binder after 7, 14, and 28 days were 590.0 kPa, 789.85 kPa, and 1050.26 kPa, respectively. These values represent increases of 45.8%, 51.9%, and 64.1%, respectively, compared with specimens cured at +10°C. This behaviour is attributed to the temperature-dependent nature of hydration reactions. Higher curing temperatures accelerate hydration reactions and promote the formation of cementitious products, thereby enhancing soil strength. Conversely, lower temperatures reduce the hydration reaction rate, resulting in slow strength development, as also reported by Calik and Sadoglu [63].

Figure 6 presents the relationship between vertical pressure and shear strength for BA-LC³ binder-stabilised BCS at curing temperatures of +10°C and+32°C. The results indicate that shear strength increased with both vertical pressure and binder content. Based on linear regression analysis of the shear strength-vertical pressure relationship, the Mohr-Coulomb failure criterion, shown in Equation (2), was used to evaluate the shear strength parameters:

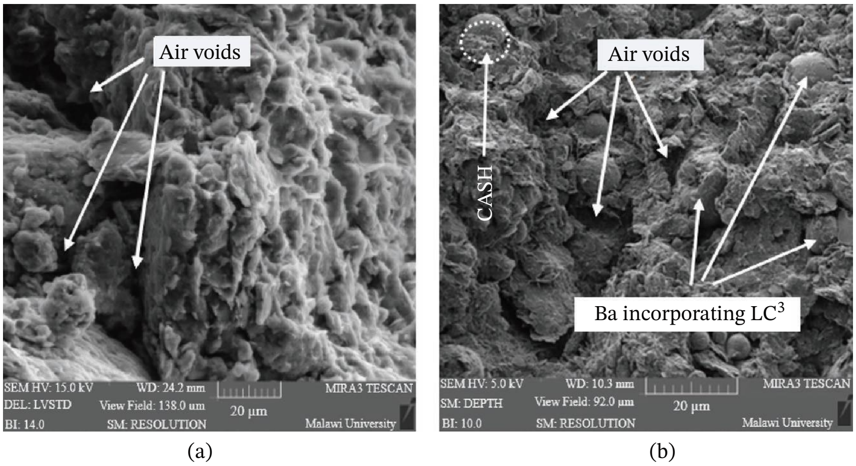


**FIGURE 5** | SEM images at 20 $\mu m$ for specimens cured at 28 days: (a) untreated BCS and (b) 18% BA-LC$^3$ binder-treated BCS.

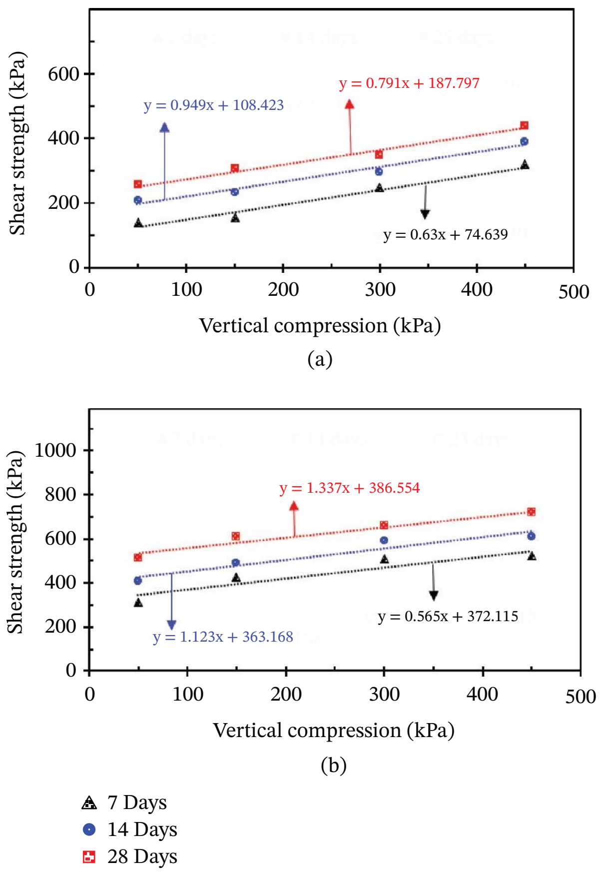


**FIGURE 6** | Variation in shear strength–vertical pressure of BA-LC$^3$ binder-treated BCS at different curing temperatures: (a) at +10°C curing temperature and (b) at +32°C curing temperature.

$$\tau = c + \sigma \tan \varphi \tag{2}$$

Where:

$\tau$ = shear strength.

$c$ = cohesion.

$\sigma$ = normal stress (vertical pressure).

$\varphi$ = internal friction angle.

Figure 7 illustrates the variation of internal friction angle with BA-LC$^3$ binder content at different curing temperatures. At +10°C, the internal friction angle increased with binder content for specimens cured at 7 and 14 days. However, for specimens cured at 28 days, the internal friction angle initially increased and subsequently decreased at higher binder contents. A similar trend was observed at +32°C, where the internal friction angle increased initially and then decreased beyond a certain binder content. These results indicate that an optimum binder content exists for maximising the internal friction angle. In this study, the optimum BA-LC$^3$ binder content was approximately 15% for both curing temperatures. This behaviour can be explained by the formation of hydration products that fill soil pores and enhance interparticle bonding (Figure 5). However, excessive binder content may lead to microstructural stiffness and brittle behaviour, resulting in reduced frictional resistance.

Figure 8 shows the relationship between BA-LC$^3$ binder content and cohesion of treated BCS. The results indicate that cohesion increased with increasing binder content and curing period. This behaviour can be attributed to the continuous formation and accumulation of hydration products, which enhance bonding between soil particles. As hydration progresses, the soil structure becomes more compact and cohesive, leading to increased shear resistance.

To evaluate the influence of dry density on the shear behaviour of treated BCS, dry densities of 16.31, 16.37, 16.43, 16.49, and 16.55 kN/m$^3$ were selected based on the compaction results presented in Table 2. Figures 9 and 10 illustrate the effect of dry density on the shear strength of BA-LC$^3$ binder-treated BCS at curing temperatures of +10°C and+32°C, respectively. Regardless of curing temperature, shear strength increased with increasing dry density. This improvement can be attributed to the reduction of interparticle voids and pore

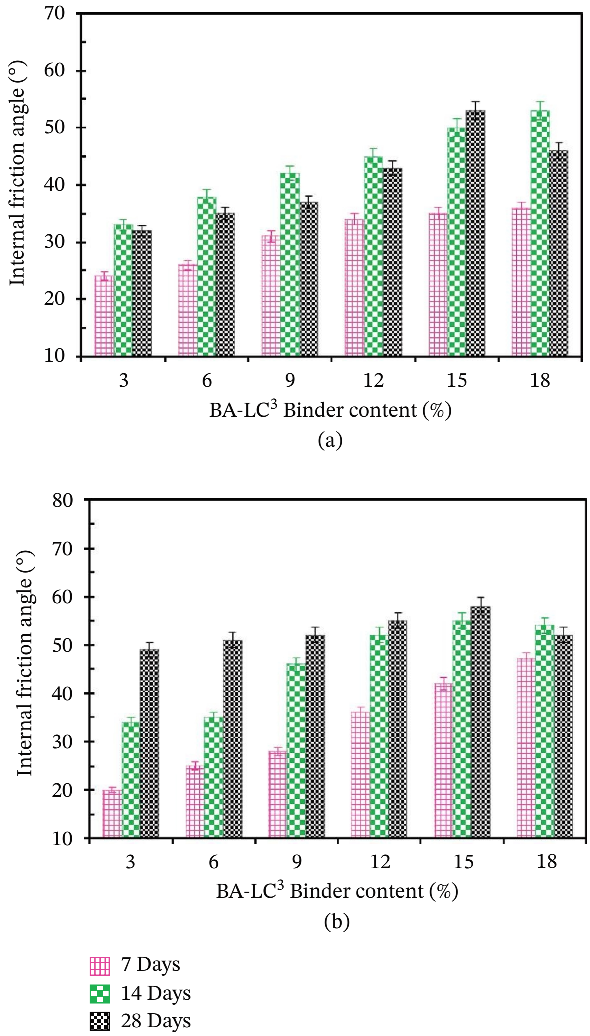


**FIGURE 7** | Effect of BA-LC$^3$ binder content on internal friction angle of treated BCS at different curing temperatures: (a) at +10°C curing temperature and (b) at +32°C curing temperature.

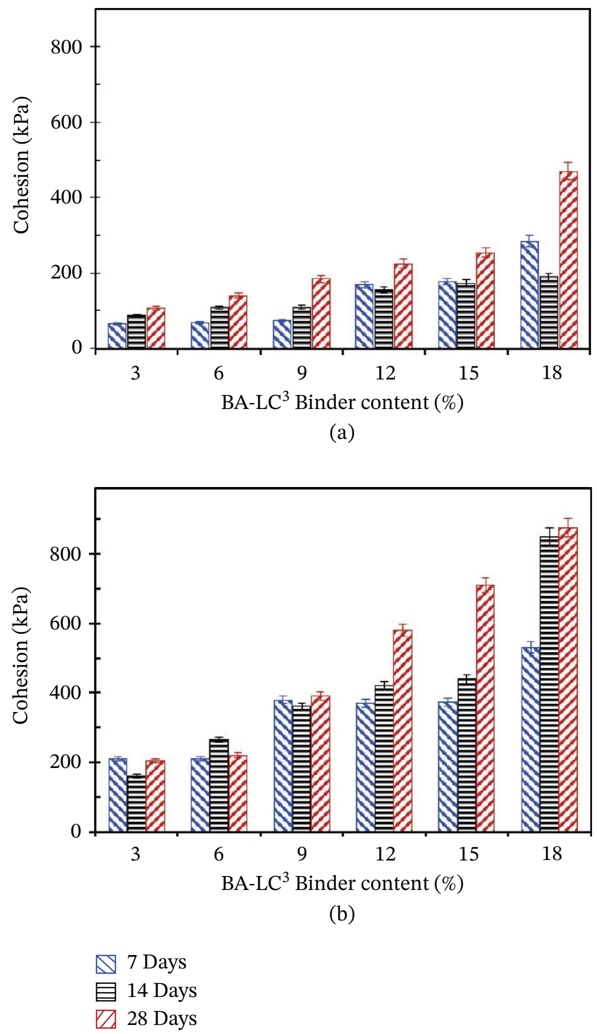


**FIGURE 8** | Effect of BA-LC$^3$ binder content on cohesion of treated BCS at different curing temperatures: (a) at +10°C curing temperature and (b) at +32°C curing temperature.

sizes, which enhances soil compactness. The formation of hydration products further strengthens particle bonding, thereby improving the structural integrity and shear resistance of the treated soil.

Figures 11 and 12 depict the impact of curing temperature on shear strength of treated BCS at various BA-LC$^3$ binder contents and dry densities, respectively. Shear strength of BA-LC$^3$ binder-treated BCS cured at +10°C temperature is minimal as compared with the shear strength of BA-LC$^3$ binder-treated BCS cured at +32°C temperature. This phenomenon was attributed to different curing temperatures, with low temperature inhibiting the rate of hydration reaction. Thus, high-temperature curing facilitated the hydration reaction rate, consequently strengthening cementation of treated BCS particles, hence shear strength enhancement. This finding corresponds well with findings by Abdullah et al. [22] and Lee et al. [67].

## 3.2 | Triaxial Shear Behaviour

To further evaluate the mechanical behaviour of the stabilised soil, triaxial tests were conducted on untreated BCS and BCS treated with 15% BA-LC$^3$ binder, which corresponded to the optimum binder content. The tests were performed under confining pressures ranging from 50 kPa to 1000 kPa after 28 days of curing. The results were analysed in terms of deviatoric stress-axial strain relationship and volumetric strain-axial strain relationship.

Figure 13 shows the relationship between deviatoric stress ($q = \sigma_1 - \sigma_3$) and axial strain ($\varepsilon_1$) of untreated and treated BCS. It has to be mentioned that in this section, the response of $q = \sigma_1 - \sigma_3$ is given as $\varepsilon_1$, in which $\sigma_1$ and $\sigma_3$, respectively, depict axial and radial principal stresses. Conversely, the response of stress–strain captures its strength and deformation traits. Based on Figure 12, the stress–strains of all samples demonstrate a linear increase in $\sigma_1 - \sigma_3$ at early strains such as at $\varepsilon_1 < 3.51\%$ for untreated BCS (Figure 13a), and $\varepsilon_1 < 2.38\%$ for treated BCS (Figure 13b), indicating the initial contraction zone. Maximum $\sigma_1 - \sigma_3$ of all samples notably increased with an increase in confining pressure. For example, maximum $\sigma_1 - \sigma_3$ of treated BCS was compared under 450 and 1000 kPa confining pressures at $\varepsilon_1 = 4\%$ (Figure 12b), and results showed a 77.27% increase in maximum $\sigma_1 - \sigma_3$. Moreover, Figure 13a shows that untreated BCS exhibited higher maximum $\sigma_1 - \sigma_3$

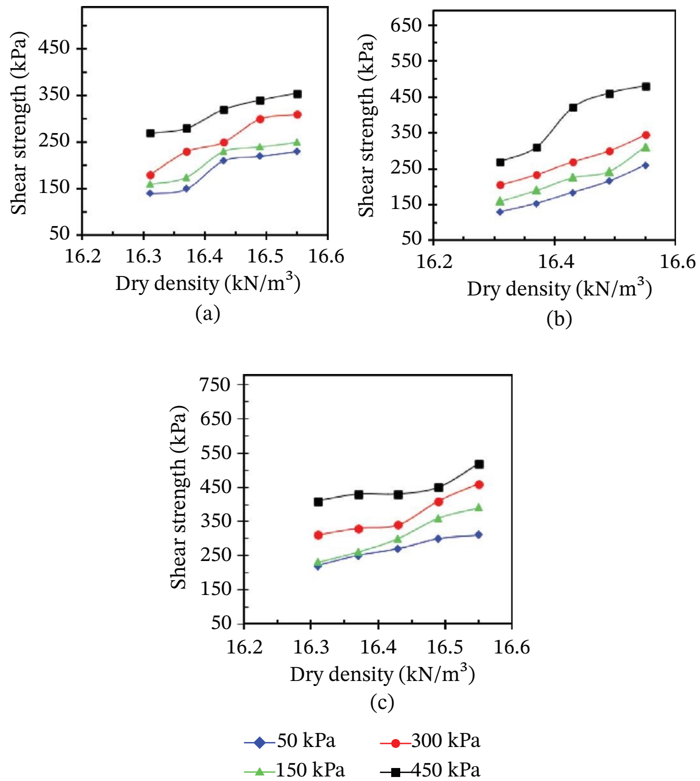


**FIGURE 9** | Effect of dry density on shear strength of treated BCS at +10°C curing temperature: (a) 7 curing days, (b) 14 curing days and (c) 28 curing days.

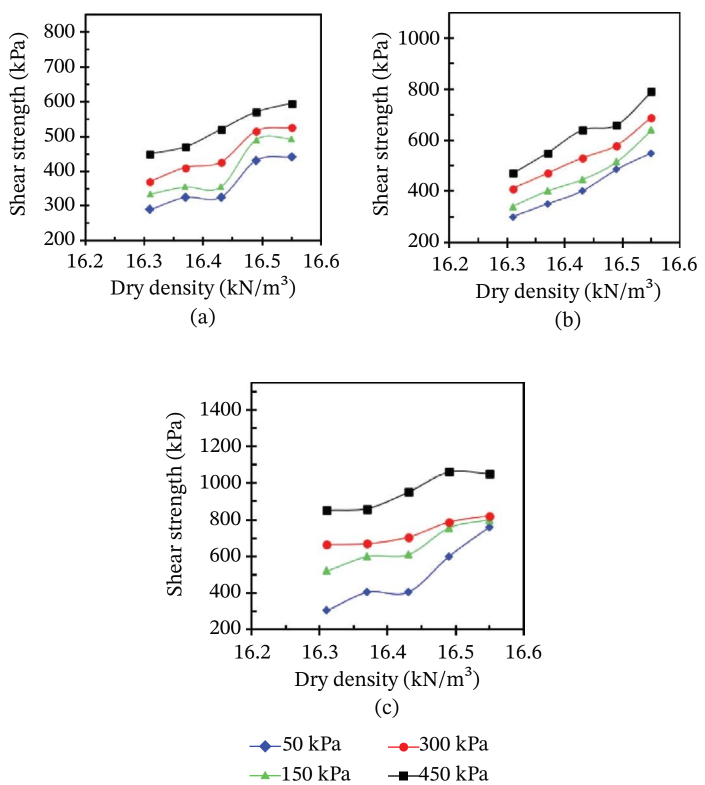


**FIGURE 10** | Effect of dry density on shear strength of treated BCS at +32°C curing temperature: (a) 7 curing days, (b) 14 curisng days and (c) 28 curing days.

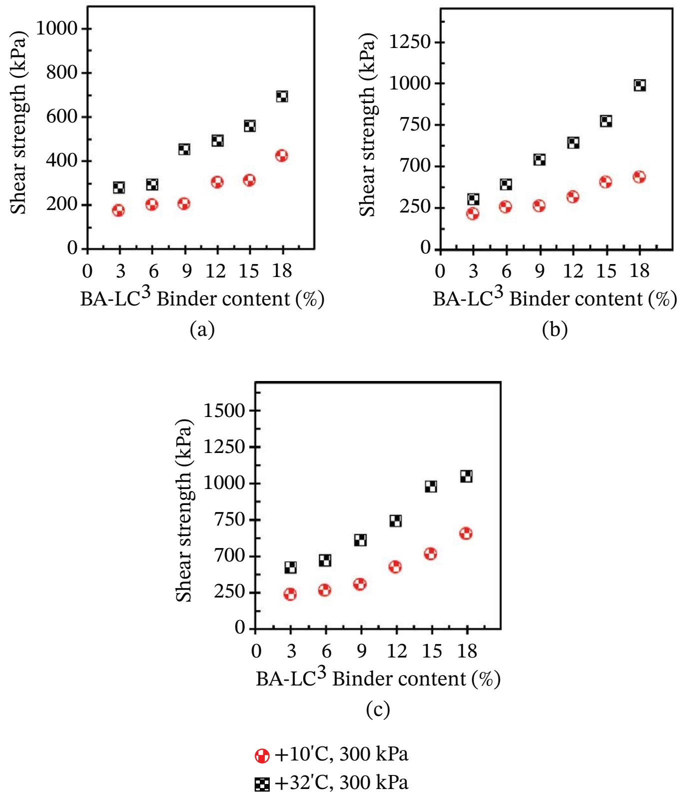


**FIGURE 11** | Effect of curing temperature on shear strength of treated BCS with various BA-LC$^3$ binder content at different curing periods: (a) 7 curing days, (b) 14 curing days and (c) 28 curing days.

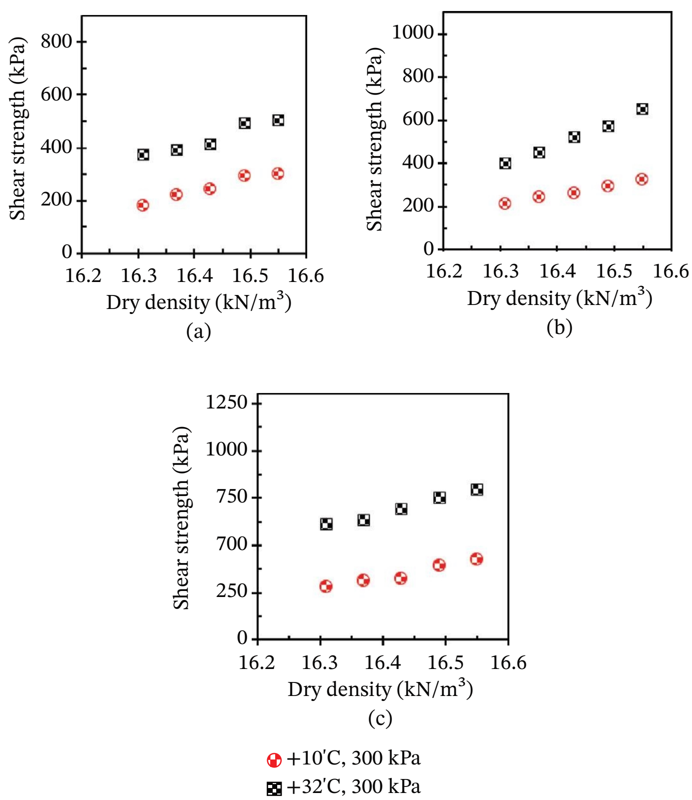


**FIGURE 12** | Effect of curing temperature on shear strength of treated BCS with various dry densities at different curing periods: (a) 7 curing days, (b) 14 curing days and (c) 28 curing days.

in comparison with treated BCS when 600-kPa confining pressure was exceeded. For instance, maximum $\sigma_1 - \sigma_3$ of untreated BCS under 600 kPa confining pressure was compared with that under 750-kPa confining pressure at $\varepsilon_1 = 14\%$ (Figure 13a). The maximum $\sigma_1 - \sigma_3$ increased from 1751.5 kPa to 2817.3 kPa, representing 60.85% increase. In contrast, under the same 600- and 750-kPa confining pressures at $\varepsilon_1 = 14\%$ for treated BCS (Figure 13b), the maximum $\sigma_1 - \sigma_3$ increase for untreated BCS reduced by 32.07%. This implies that the effect of confining pressure at higher than 600 kPa on untreated BCS was more distinct in comparison with that of treated BCS. Therefore, with an increase in confining pressure, untreated BCS underwent serious particle fragmentation, leading to structural reorganisation, and thus limited strength improvement. Conversely, all treated BCS underwent consistent mechanical performance. With an increase in confining pressure, maximum $\sigma_1 - \sigma_3$ of treated BCS improved, resulting in notable mechanical response as a result of cementation degree and fragmentation level of BCS particles. As observed in Figure 13b, postyielding strain-softening behaviour was noticed at low confining pressure, such as less than 600 kPa. On the contrary, postyielding strain-hardening response was noticed at high confining pressure, such as more than 600 kPa. Fragmentation and cementation degree of specimens played a significant role in these transition responses. Thus, under low confining pressure, the behaviour of treated BCS became more brittle, with primary loading resistance mainly due to spatial bonding strength. With high confining pressure, strength of treated BCS was mainly attributed to strength of particles, particle fragmentation and rearrangement. This suggests that particle fragmentation dominated the mechanical response of treated soils after attaining maximum $\sigma_1 - \sigma_3$ in the triaxial test, as previously discovered by Lyu et al. [68].

Moreover, shear behaviour of BCS is more attributed to volumetric strain $(\varepsilon_v)$ changes, where negative and positive changes correlate with dilation and compression of samples during the stage of shearing. It is mostly reported that notable changes in dilative $\varepsilon_v$ are very significant during substantial axial strain $(\varepsilon_1)$, low conditions of confining pressure, and higher stress levels close to failure [64]. Similarly, at less than 600 kPa confining pressure, untreated and treated BCS showed contraction at low $\varepsilon_1$ of about 3.51% (Figure 14a) and 2.03% (Figure 14b), respectively, succeeded by successive solid dilation. Besides, at 50 kPa confining pressure, differences in $\varepsilon_v$ for untreated and treated

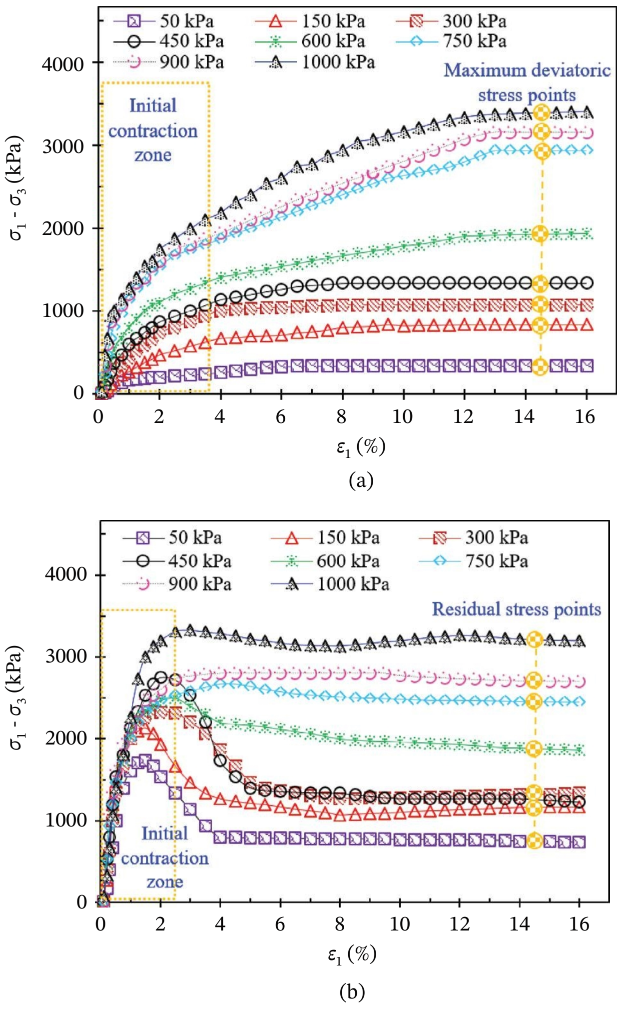


**FIGURE 13** | Variation in deviatoric stress–axial strain under various confining pressures: (a) untreated BCS and (b) 15% BA-LC³ binder-treated BCS.

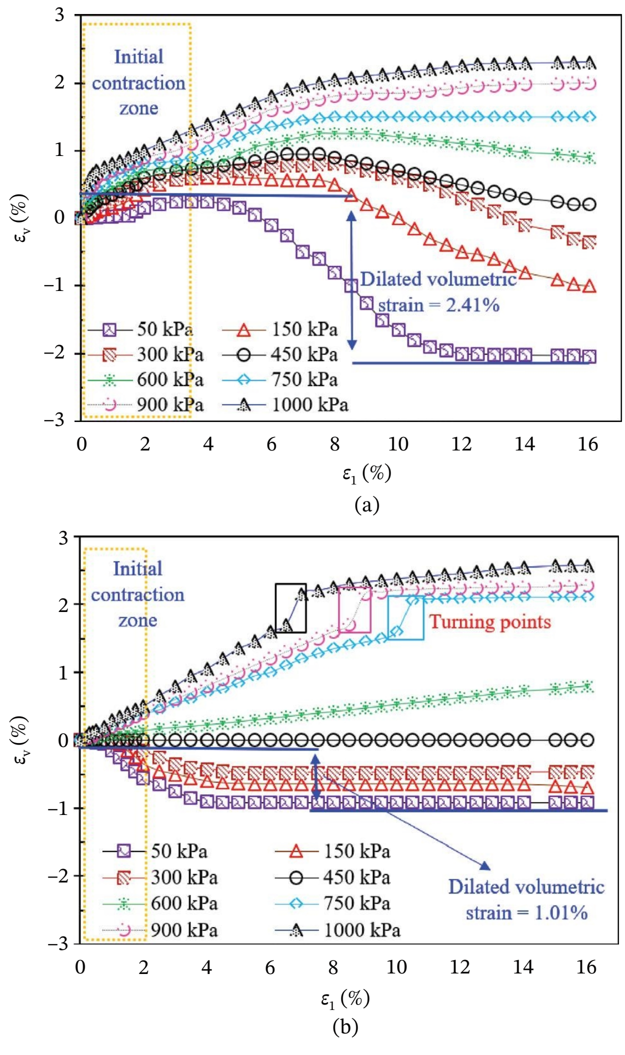


**FIGURE 14** | Variation in volumetric strain–axial strain under various confining pressures: (a) untreated BCS and (b) 15% BA-LC³ binder-treated BCS.

BCS were about 2.41% (Figure 14a) and 1.01% (Figure 14b), respectively. Likewise, 15% BA-LC[3] binder content weakened the dilatancy properties of BCS, whereby the hydration products integrated BCS into a compact entity, decreasing particle amount and, hence, resulting in dilatancy behaviour. This further implies that treated BCS particles exhibited notable curtailment against rearranging, tumbling, sliding and overturning caused by the effect of bonding, particularly at low stress levels, thereby possibly crippling the dilatancy behaviour. Besides, values of dilative $\varepsilon_v$ decreased with increasing confining pressure to a point of stress–strain curve, demonstrating an absolute shear contraction. This finding reveals that $\varepsilon_1$ level and corresponding maximum $\sigma_1 - \sigma_3$ increased with an increase in confining pressure. Parallel conclusion was drawn by Azneb et al. [69].

Figure 15 summarises the maximum $\sigma_1 - \sigma_3$ principal stress ratio of treated BCS. With an increase in confining pressure, the maximum principal stress ratio reduces. To illustrate, it was previously shown that beyond coloured rectangular turning points (Figure 14b), stress–strain behaviour of treated BCS deteriorates to that of untreated BCS (Figure 14a). This suggests that shear strength and bond stiffness became virtually zero at high confining pressure. Thus, bonding strength and structural interlocking of treated BCS partially sustained loading capacity and provided limited influence on strength improvement. To better demonstrate this phenomenon, maximum $\sigma_1 - \sigma_3$ of untreated and treated BCS is plotted in Figure 16. As confining pressure increases, the point of maximum $\sigma_1 - \sigma_3$ approached a zone above untreated BCS failure envelope, intersected it, and remained parallel to it, hence, further corroborating findings portrayed in Figure 15. Therefore, when using 15% BA-LC[3] binder content to improve the strength of BCS relevant to geotechnical foundations, it is important to scrupulously evaluate the potential effects of high-pressure conditions.

### 3.3 | Grey Relational Analysis

With regard to the obtained shear strength results in this study, several factors impact the shear behaviour of BA-LC[3] binder-treated BCS. Hence, it is very essential to rank factors that affect shear strength of BA-LC[3] binder-treated BCS for the purpose of designing, construction and rehabilitation of geotechnical structures founded on BCS, specifically for regions that experience tropical climatic conditions such as Shire Valley. In this section, a grey relational analysis was employed to establish the degree to which each variable impacted targeted results, in consideration of multiple independent variables. According to Feng et al. [70], the coefficient of correlation of reference sequence $Y_o$ (shear strength behaviour) and comparative sequences $Y_i$ (influencing factors, in this case BA-LC[3] binder content, dry density, curing period and curing temperature) at $N$ point can be expressed as follows:

$$\lambda_i(N) = \frac{\left[\min_i \min_N |Y_i(N) - Y_o(N)| + \beta \max_i \max_N |Y_i(N) - Y_o(N)|\right]}{\left[|Y_i(N) - Y_o(N)| + \beta \max_i \max_N |Y_i(N) - Y_o(N)|\right]}, \quad (3)$$

where

$\lambda_i(N)$ = coefficient of correlation;

$|Y_i(N) - Y_o(N)|$ = absolute variation in comparison column between reference column and correlating data;

$\beta = 0.5$ resolution coefficient [70];

$\max_i \max_N |Y_i(N) - Y_o(N)|$ = highest values in absolute difference;

$\min_i \min_N |Y_i(N) - Y_o(N)|$ = lowest values in absolute difference.

Thus, the correlation degree between the sequence of reference and comparison can be computed as

$$X_i = \frac{1}{h} \sum_{i=1}^{h} \lambda_i(N), \quad (4)$$

where

$X_i$ = correlation degree in the range of 0 to 1, in which $Y_i$ strongly impacts $Y_o$ if the correlation degree is higher;

$h$ = number of analysed data.

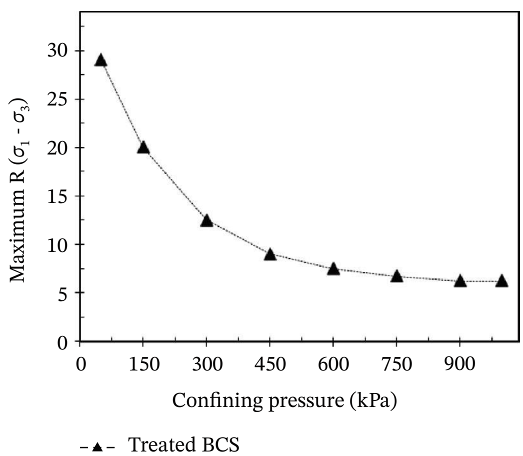


**FIGURE 15** | Similarity between confining pressure and maximum principal stress ratio for 15% BA-LC[3] binder-treated BCS.

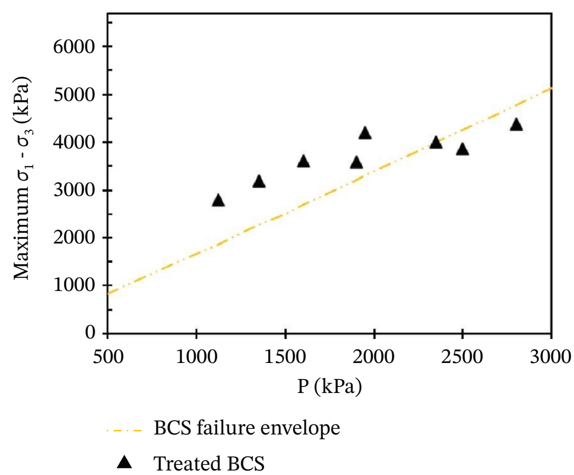


**FIGURE 16** | Points of maximum deviatoric stress under different confining pressures for 15% BA-LC[3] binder-treated BCS.

Figure 17 presents the correlation degree between shear strength and influencing factors over various ranges of vertical pressures. BA-LC³ binder content, dry density and curing period firmly correlated with shear strength, with a correlation degree of more than 0.7 on average. Hence, these three factors remarkably impacted the shear strength of BA-LC³ binder-treated BCS. However, the correlation degree between shear strength and curing temperature was lowest (about 0.513 on average). Thus, curing temperature posed a proportionally weak impact on shear strength. Hence, relative measures, such as increasing BA-LC³ binder additive content, should be used within an acceptable range of cost to improve shear strength of BA-LC³ binder-treated BCS in tropical regions. Besides, the correlation degree between cohesion and internal friction angle with other influencing factors such as BA-LC³ binder content, curing period and curing temperature is portrayed in Figure 18. It can be seen that cohesion and internal friction angle were coherent based on correlation degree. The correlation degree of cohesion and internal friction angle against BA-LC³ binder content was highest, superseded by curing period and curing temperature. This pointed to the fact that hydration products were the most outstanding factors that impacted the strength performance of BA-LC³ binder-treated BCS.

## 3.4 | Ecological and Cost Analysis

To assess carbon footprint and cost for BCS treatment with BA-LC³ binder, 1.0 t of treated BCS was considered in Shire Valley, Malawi. The carbon footprint and cost estimations were calculated based on comparative analysis with that of treated BCS with traditional OPC binder. Mix design of treating 1.0 t of BCS with BA-LC³ binder and OPC binder is given in Table 4. Ecological assessments were performed using life cycle inventory analysis in accordance with ISO 14040 [71]. Two parameters, integrated energy (IE) and integrated carbon footprint (ICF), were introduced. IE stands for the consumed energy amount, whereas ICF denotes $CO_2$ emissions during raw material extraction, transportation and manufacturing [72]. Table 5 presents parameter coefficients of IE and ICF for adopted raw materials based on the eco-inventory database and literature [73–75]. The cost of BA, LC³ and OPC materials was analysed with regard to current prices of materials in Malawi, converted into US dollars ($). It has to be mentioned that the costs of materials are inherently variable and subject to change over time. Therefore, to extensively evaluate the ecological and economic efficiency of mixtures, the IE, ICF and cost of mixtures were calculated and compared as presented in Figure 19. BA-LC³ binder-treated BCS has the smallest values of IE, ICF and cost, indicating 1010.1 J/t (Figure 19a), 111.51 kg-$CO_2$/t (Figure 19b) and 19.89$/t (Figure 19c), respectively. Compared with OPC binder-treated BCS, the IE, ICF and cost of BA-LC³ binder-treated BCS reduced by 14.6% (Figure 19a),

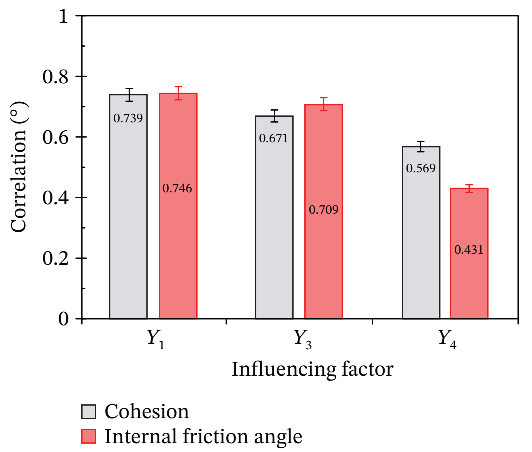


**FIGURE 18** | Correlation degree between influencing factors and shear strength parameters.

**TABLE 4** | Mix design of binders for 1.0-t dry BCS.

| Material | BA incorporating LC³ | OPC |
|---|---|---|
| BA (kg) | 126 | — |
| LC³ (kg) | 84 | — |
| OPC (kg) | — | 210 |

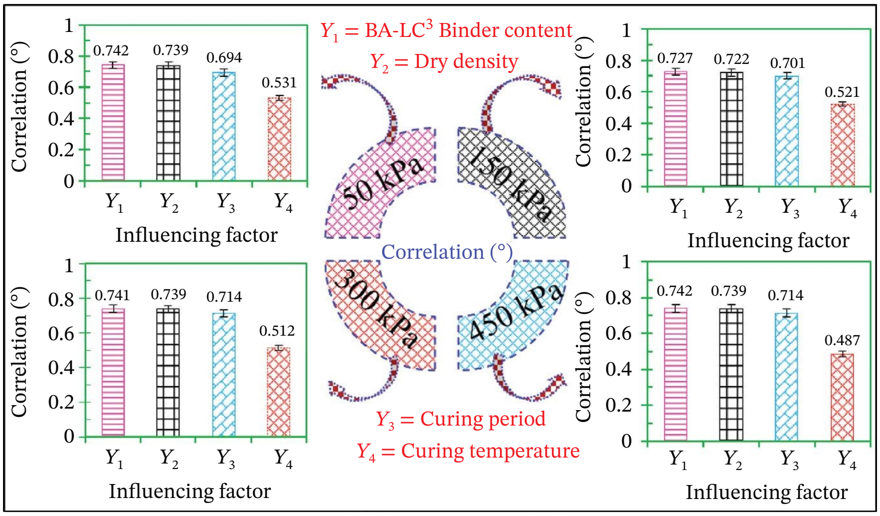


**FIGURE 17** | Correlation degree between shear strength and influencing factors under various vertical pressures.

**TABLE 5** | Basic parameter coefficients of IE, ICF and cost for BA-$LC^3$ component materials and OPC material used for BCS stabilisation technique.

| Material | IE (KJ/t) | ICF ($t\,CO_2/t$) | Avg. Cost ($/t) |
|---|---|---|---|
| BA | 1.02 | 0.101 | 1.26 |
| Limestone (LS) | 0.84 | 0.033 | 32.10 |
| Calcined clay (CC) | 2.73 | 0.195 | 43.15 |
| Ground clinker (CL) | 5.51 | 0.719 | 149.26 |
| Gypsum (Gyp) | 1.79 | 0.120 | 21.40 |
| OPC | 5.51 | 0.907 | 161.47 |

Abbreviations: Avg. Cost ($/t) = average total cost to produce, handle or transport 1 t of material based on current prices of materials in Malawi, converted into US dollars; ICF ($t\,CO_2/t$) = total greenhouse gas emissions generated per unit of output; IE (KJ/t) = total specific energy input per metric tonne.

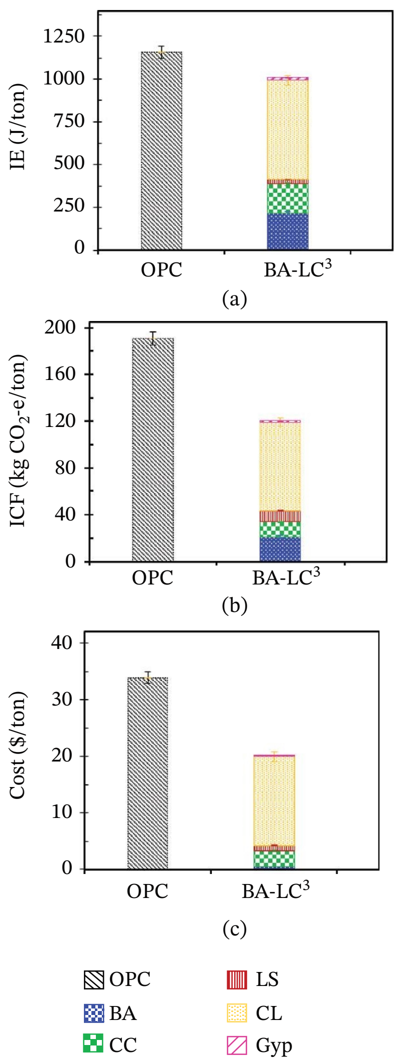


**FIGURE 19** | Ecological and cost implications of using BA-$LC^3$ on BCS stabilisation compared with using traditional OPC: (a) integrated energy, (b) integrated carbon footprint and (c) cost.

70.8% (Figure 19b) and 70.5% (Figure 19c), respectively. This reveals that BA-$LC^3$ binder-treated BCS has the most remarkable economic and ecological efficiency. Conversely, OPC binder-treated BCS has a higher impact on the IE, ICF and cost. Hence, on a large scale, a significant amount of cost can be saved, and the carbon footprint can be reduced with the use of the BA-$LC^3$ binder technique for the stabilisation of BCSs. This further implies that BA-$LC^3$ binder is one of the cleaner and cost-effective promising options for treatment of BCS relevant to geotechnical applications in Shire Valley, Malawi.

## 4 | Conclusion

This study evaluated the influence of BA-$LC^3$ binder on the shear behaviour of BCS in Shire Valley, Malawi, which experiences tropical climatic conditions. Based on the experimental results, the following conclusions were drawn:

1. Due to the adhesion of cementitious products to BCS particles, the direct shear strength of BA-$LC^3$ binder-treated BCS significantly increased with increasing BA-$LC^3$ binder content, dry density, curing period and curing temperature. The peak SSD values of BA-$LC^3$ binder-treated BCS increased with higher vertical pressures. In addition, the failure patterns of untreated BCS and BA-$LC^3$ binder-treated BCS were notably different. Untreated BCS exhibited ductile failure, whereas BA-$LC^3$ binder-treated BCS showed brittle failure behaviour. The direct shear strength results confirm the effectiveness of the BA-$LC^3$ binder in improving the mechanical properties of BCS, which can contribute to the reliability and stability of foundation soils in tropical regions.
2. The triaxial test results showed significant volumetric strain variations in BA-$LC^3$ binder-treated BCS under low confining pressures and large axial strains. As the confining pressure increased, contraction became more dominant while dilation decreased. Stress–strain hardening was associated with considerable axial strains at the points of maximum deviatoric stress. Furthermore, the volumetric strain corresponding to the maximum principal stress ratio increased with increasing confining pressure, mainly due to particle fragmentation and shear dilation in BA-$LC^3$ binder-treated BCS. The findings from the triaxial shear strength tests are consistent with those obtained from the direct shear strength tests. Overall, the direct and triaxial shear behaviour, together with the BA-$LC^3$ binder content, provide valuable insights into the behaviour of stabilised BCS and improve the understanding of the BCS stabilisation mechanism.
3. With large-scale use of the BA-$LC^3$ binder technique on the stabilisation of BCS, a significant amount of cost can be saved and the carbon footprint can be reduced, aligning with efforts to address climate change impacts and reduce infrastructure development costs.

In this study, CD direct shear strength tests and triaxial compression shear strength tests were conducted to evaluate the effects of BA-$LC^3$ binder content, curing period, dry density, vertical pressure and curing temperature on BCS behaviour. The influence of different static loading conditions on the shear strength performance of treated BCS was also assessed. These investigations contribute to the existing body of knowledge by identifying key factors for effective BCS stabilisation in tropical regions. Future studies should consider additional geotechnical construction conditions that were not examined in this study, such as consolidation, durability and fatigue tests, not only in tropical regions but also in other environments, including cold regions. Failure patterns considering the influence of bonding strength should also be comprehensively examined to quantitatively provide deep insights into the failure criteria of BA-$LC^3$ binder-treated BCS. Further research may also explore other problematic soil types and BA and $LC^3$ materials sourced from locations beyond the Shire Valley in Malawi. Such studies would help to comprehensively evaluate the feasibility of BA-$LC^3$ binder for stabilising BCS and other problematic soils, thereby supporting more cost-effective and sustainable geotechnical construction and infrastructure development.

### Acknowledgements

No AI software has been used in the preparation of this manuscript.

### Funding

No funding was received for this manuscript.

### Disclosure

No unlisted individuals or third-party services were involved in the research or manuscript preparation, and all authors have read and approved the contents of the manuscript.

### Conflicts of Interest

The authors declare no conflicts of interest.

### Data Availability Statement

This article includes the data used to support the findings.

### References

1. Y. Izumi, A. Iizuka, and H. J. Ho, "Calculation of Greenhouse Gas Emissions for a Carbon Recycling System Using Mineral Carbon Capture and Utilization Technology in the Cement Industry," *Journal of Cleaner Production* 312 (2021): 127618, https://doi.org/10.1016/j.jclepro.2021.127618.

2. N. Mohamad, K. Muthusamy, R. Embong, A. Kusbiantoro, and M. H. Hashim, "Environmental Impact of Cement Production and Solutions: A Review," *Materials Today Proceedings* 48 (2022): 741–746, https://doi.org/10.1016/j.matpr.2021.02.212.

3. N. Ijaz, W. M. Ye, Z. Rehman, Z. Ijaz, and M. F. Junaid, "Global Insights into Micro-Macro Mechanisms and Environmental Implications of Limestone Calcined Clay Cement (LC3) for Sustainable Construction Applications," *Science of the Total Environment* 907 (2024): 167794, https://doi.org/10.1016/j.scitotenv.2023.167794.

4. M. S. Imbabi, C. Carrigan, and S. McKenna, "Trends and Developments in Green Cement and Concrete Technology," *International Journal of Sustainable Built Environment* 1, no. 2 (2012): 194–216, https://doi.org/10.1016/j.ijsbe.2013.05.001.

5. K. L. Scrivener, V. M. John, and E. M. Gartner, "Eco-Efficient Cements: Potential Economically Viable Solutions for a Low $CO_2$ Cement Based Materials Industry," *Cement and Concrete Research* 114 (2018): 2–26, https://doi.org/10.1016/j.cemconres.2018.03.015.

6. C. Shi, A. F. Jiménez, and A. Palomo, "New Cements for the 21st Century: The Pursuit of an Alternative to Portland Cement," *Cement and Concrete Research* 41, no. 7 (2011): 750–763, https://doi.org/10.1016/j.cemconres.2011.03.016.

7. G. Schiller, and J. Roscher, "Impact of Urbanization on Construction Material Consumption: A Global Analysis," *Journal of Industrial Ecology* 27 (2023): 1021–1036, https://doi.org/10.1111/jiec.13392.

8. M. Nuruddin, A. A. B. Moghal, R. M. Rasheed, G. G. K. Sravya, R. Balaramakrishna, and Y. Vyshnavi, "Coupled Effect of Ground Granulated Blast Slag and Bagasse Fibers to Enhance the Compressive Strength and Durability Characteristics of Expansive Soil," *Geotechnical Frontiers* 363 (2025): 323–331, https://doi.org/10.1061/9780784485965.029.

9. S. Himani, J. Kitendra, and A. Biswajit, "Stabilization of Black Cotton Soil by Using Sugarcane Bagasse Ash," *International Journal of Scientific Research and Review* 7, no. 1 (2019): .

10. A. Maneli, W. K. Kupolati, O. S. Abiola, and J. M. Ndambuki, "Influence of Fly Ash, Ground-Granulated Blast Furnace Slag and Lime on Unconfined Compressive Strength of Black Cotton Soil," *Road Materials and Pavement Design* 17, no. 1 (2016): 252–260, https://doi.org/10.1080/14680629.2015.1066703.

11. M. J. Aliyu, L. Z. Adam, and S. U. Kunya, "Investigating the Engineering Properties of Black Cotton Soil Treated With Rice Husk Ash," *African Scholar Journal of Environmental Design and Construction Management* 18, no. 4 (2020): .

12. P. Ghadira, and N. Ranjbar, "Clayey Soil Stabilization Using Geopolymer and Portland Cement," *Construction and Building Materials* 188 (2018): 361–371, https://doi.org/10.1016/j.conbuildmat.2018.07.207.

13. S. Patil, D. A. Joshi, R. Menon, and L. Wadhwa, "Environmental Impact Assessment of Fly Ash and GGBS-Based Geopolymer Concrete in Road Construction," *E3S Web of Conference* 5 (2023): 3021, https://doi.org/10.1051/e3sconf/202340503021.

14. B. C. McLellan, R. P. Williams, J. Lay, A. V. Riessen, and G. D. Corder, "Costs and Carbon Emissions for Geopolymer Pastes in Comparison to Ordinary Portland Cement," *Journal of Cleaner Production* 19, no. 9-10 (2011): 1080–1090, https://doi.org/10.1016/j.jclepro.2011.02.010.

15. M. Ashfaq, and A. A. B. Moghal, "Cost and Carbon Footprint Analysis of Flyash Utilization in Earthworks," *International Journal of Geosynthetics and Ground Engineering* 8, no. 2 (2022): , https://doi.org/10.1007/s40891-022-00364-4.

16. W. J. Longa, Z. Wu, K. H. Khayat, et al., "Design, Dynamic Performance and Ecological Efficiency of Fiber-Reinforced Mortars With Different Binder Systems: Ordinary Portland Cement, Limestone Calcined Clay Cement and Alkali-Activated Slag," *Journal of Cleaner Production* 337 (2022): 130478, https://doi.org/10.1016/j.jclepro.2022.130478.

17. A. A. B. Moghal, B. Chittoori, B. M. Basha, and A. Mahbashi, "Effect of Polypropylene Fibre Reinforcement on the Consolidation, Swell and Shrinkage Behaviour of Lime-Blended Expansive Soil," *International Journal of Geotechnical Engineering* 5, no. 5 (2017): 462–471, https://doi.org/10.1080/19386362.2017.1297002.

18. D. Shi, Y. Xia, J. Wang, et al., "Recycling E-Waste CRT Glass in Sustainable Geopolymer Concrete for Radiation Shielding Applications," *Journal of Environmental Chemical Engineering* 12, no. 6 (2024): 114693, https://doi.org/10.1016/j.jece.2024.114693.

19. H. Achak, M. R. Sohrabi, and S. O. Hoseini, "Effects of microsilica and Polypropylene Fibers on the Rheological Properties, Mechanical Parameters and Durability Characteristics of Green Self-Compacting Concrete Containing Ceramic Wastes," *Construct Build Mater* 392 (2023): 131890, https://doi.org/10.1016/j.conbuildmat.2023.131890.

20. A. Aghaeipour, and M. Madhkhan, "Effect of Ground Granulated Blast Furnace Slag (GGBFS) on RCCP Durability," *Construction*

*Building Materials* 141 (2017): 533–541, https://doi.org/10.1016/j.conbuildmat.2017.03.019.

21. N. S. Pandian, K. C. Krishna, D. Petersen, and R. Link, "The Pozzolanic Effect of Fly Ash on the California Bearing Ratio Behavior of Black Cotton Soil," *Journal of Testing and Evaluation* 31, no. 6 (2003): 479–485, https://doi.org/10.1520/JTE12375J.

22. H. Abdullah, M. A. Shahin, and P. Sarker, "Use of Fly-Ash Geopolymer Incorporating Ground Granulated Slag for Stabilisation of Kaolin Clay Cured at Ambient Temperature," *Geotechnical and Geological Engineering* 37, no. 2 (2019): 721–740, https://doi.org/10.1007/s10706-018-0644-2.

23. L. A. Sofri, M. Abdullah, A. V. Sandu, et al., "Mechanical Performance of Fly Ash Based Geopolymer (FAG) as Road Base Stabilizer," *Materials* 15, no. 20 (2022): 7242, https://doi.org/10.3390/ma15207242.

24. N. Wu, T. Ji, P. Huang, T. Fu, X. Zheng, and Q. Xu, "Use of Sugar Cane Bagasse Ash in Ultra-High-Performance Concrete (UHPC) as Cement Replacement," *Construction and Building Materials* 317 (2022): 125881, https://doi.org/10.1016/j.conbuildmat.2021.125881.

25. P. K. Amrutha, K. S. Muthu, V. B. Vaishnavi, S. S. Mahesh, and P. Aavani, "Black Cotton Soil Stabilization Using Bagasse Ash and Lime," *International Journal of Civil Engineering and Technology (IJCIET)* 67, no. 6 (2016): 460–471.

26. H. K. Nangulama, and W. Kuotcha, "Efficiency of Bagasse Ash Incorporated With Limestone Calcined Clay Cement on Improvement of Geotechnical Properties of Black Cotton Soils: A Cleaner Approach," *Journal of Engineering* 2025, no. 1 (2025): 2225558, https://doi.org/10.1155/je/2225558.

27. N. H. Serker, R. U. Hafiz, A. H. Rahman, and M. Ashikuzzaman, "Suitability of Using Sugarcane Bagasse Ash as Partial Replacement of Cement in Concrete," in *5th International Conference on Advances in Civil Engineering* (CUET, 2020).

28. P. Chindaprasirt, P. Sujumnongtokul, and P. Posi, "Durability and Mechanical Properties of Pavement Concrete Containing Bagasse Ash," *Materials Today: Proceedings* 17 (2019): 1612–1626, https://doi.org/10.1016/j.matpr.2019.06.191.

29. A. Bahurudeen, D. Kanraj, V. Gokul, and M. Santhanam, "Performance Evaluation of Sugarcane Bagasse Ash Blended Cement in Concrete," *Cement and Concrete Composites* 59 (2015): 77–88, https://doi.org/10.1016/j.cemconcomp.2015.03.004.

30. J. Bajaj, and V. K. Singh, "Performance Evaluation of Black Cotton Soil Stabilized With Sugarcane Bagasse Ash and Randomly Distributed Coir Fibres," *International Journal for Innovative Research in Science & Technology* 2, no. 11 (2016): 493–498.

31. A. Akbar, F. Farooq, M. Shafique, F. Aslam, R. Alyousef, and H. Alabduljabbar, "Sugarcane Bagasse Ash-Based Engineered Geopolymer Mortar Incorporating Propylene Fibers," *Journal of Building Engineering* 33 (2021): , https://doi.org/10.1016/j.jobe.2020.101492.

32. S. Patel, and J. T. Shahu, "Engineering Properties of Black Cotton Soil–Dolime Mix for Its Use as Subbase Material in Pavements," *International Journal of Geomate* 8, no. 1 (2015): 1159–1166, https://doi.org/10.21660/2015.15.4191.

33. B. Sudip, G. Goswami, K. Hadi, K. Moses, B. Parinita, and N. Kalita, "Comparative Study on Soil Stabilization Relevant to Transport Infrastructure Using Bagasse Ash and Stone Dust and Cost Effectiveness," *Civil Engineering Journal* 7, no. 11 (2021): , https://doi.org/10.28991/cej-2021-03091771.

34. H. Hayder, L. Dang, H. Khabbaz, B. Fatahi, and S. Terzaghi, "Remediation of Expansive Soils Using Agricultural Waste Bagasse Ash," *Procedia Engineering* 143 (2016): 1368–1375, https://doi.org/10.1016/j.proeng.2016.06.161.

35. Y. C. Díaz, S. S. Berriel, U. Heierli, et al., "Limestone Calcined Clay Cement as a Low-Carbon Solution to Meet Expanding Cement Demand in Emerging Economies," *Development Engineering* 2 (2017): 82–91, https://doi.org/10.1016/j.deveng.2017.06.001.

36. K. Scrivener, F. Martirena, S. Bishnoi, and S. Maity, "Calcined Clay Limestone Cements (LC3)," *Cement and Concrete Research* 114 (2018): 49–56, https://doi.org/10.1016/j.cemconres.2017.08.017.

37. A. Akindahunsi, F. Avet, and K. Scrivener, "The Influence of Some Calcined Clays From Nigeria as Clinker Substitute in Cementitious Systems," *Case Studies in Construction Materials* 13 (2020): , https://doi.org/10.1016/j.cscm.2020.e00443.

38. S. Joseph, S. Bishnoi, and S. Maity, "An Economic Analysis of the Production of Limestone Calcined Clay Cement in India," *Indian Concrete Journal* 90, no. 11 (2016): 22–27.

39. M. D. Sheikh, T. Jamil, T. Ayub, A. U. R. Khan, S. M. Bilal, and C. Hu, "Comparative Study on LC3-50 With OPC Concrete Using Raw Materials From Pakistan," *Advances in Materials Science and Engineering* 2023 (2023): 5503670, https://doi.org/10.1155/2023/5503670.

40. M. Sharma, S. Bishnoi, F. Martirena, and K. Scrivener, "Limestone Calcined Clay Cement and Concrete: A State-Of-The-Art Review," *Cement and Concrete Research* 149 (2021): 106564, https://doi.org/10.1016/j.cemconres.2021.106564.

41. I. Kafodya, D. Basuroy, J. M. Marangu, G. Kululanga, R. Maddalena, and V. I. Novelli, "Mechanical Performance and Physico-Chemical Properties of Limestone Calcined Clay Cement (LC3) in Malawi," *Buildings* 13, no. 3 (2023): 740, https://doi.org/10.3390/buildings13030740.

42. J. Wang, D. Shi, Y. Xia, et al., "Stabilization/Solidification of Radioactive Borate Waste via Low-Carbon Limestone Calcined Clay Cement (LC3)," *Journal of Environmental Chemical Engineering* 12, no. 3 (2024): 113129, https://doi.org/10.1016/j.jece.2024.113129.

43. V. A. Reddy, C. H. Solanki, S. Kumar, K. R. Reddy, and Y. J. Du, "New Ternary Blend Limestone Calcined Clay Cement for Solidification/Stabilization of Zinc Contaminated Soil," *Chemosphere* 235 (2019): 308–315, https://doi.org/10.1016/j.chemosphere.2019.06.051.

44. L. M. Mugambi, S. Mujombi, V. Mutai, J. R. Toeri, J. M. Marangu, and L. Valentini, "Potential of Limestone Calcined Clay Cement (LC$^3$) in Soil Stabilization for Application in Roads and Pavements Construction," *Case Studies in Construction Materials* 21 (2024): e03706, https://doi.org/10.1016/j.cscm.2024.e03706.

45. P. N. Sham, V. Gholap, and P. Kolase, "Role of Limestone Calcined Clay Cement (LC3) in Low Carbon Concrete Pavements," *Communications on Applied Nonlinear Analysis* 31 (2024): , https://doi.org/10.59287/cana.6146.

46. I. Wilińska, P. Barbara, and A. Ostrowski, "Investigation of Different Ways of Activation of Fly Ash–Cement Mixtures: Part 2—Mechanical Activation," *Journal of Thermal Analysis and Calorimetry* 149, no. 20 (2024): 11389–11406, https://doi.org/10.1007/s10973-023-12503-8.

47. A. O. Eberemu, "Evaluation of Bagasse Ash Treated Lateritic Soil as a Potential Barrier Material in Waste Containment Application," *Acta Geotechnica* 8, no. 4 (2013): 407–421, https://doi.org/10.1007/s11440-012-0204-5.

48. K. Kasama, K. Zen, and K. Iwataki, "Undrained Shear Strength of Cement Treated Soils," *Soils and Foundations* 46, no. 2 (2006): 221–232, https://doi.org/10.3208/sandf.46.221.

49. S. Vichan, and R. Rachan, "Chemical Stabilization of Soft Bangkok Clay Using the Blend of Calcium Carbide Residue and Biomass Ash," *Soils and Foundations* 2, no. 53 (2013): 272–281, https://doi.org/10.1016/j.sandf.2013.02.007.

50. M. Suzuki, T. Fujimoto, and T. Taguchi, "Peak and Residual Strength Characteristics of Cement-Treated Soil Cured Under Different

Consolidation Conditions," *Soils and Foundations* 54, no. 4 (2014): 687–698, https://doi.org/10.1016/j.sandf.2014.06.023.

51. L. Nguyen, B. Fatahi, and H. Khabbaz, "Development of a Constitutive Model to Predict the Behavior of Cement-Treated Clay During Cementation Degradation: C3 Model," *International Journal of Geomechanics* 17, no. 7 (2017): , https://doi.org/10.1061/(ASCE)GM.1943-5622.0000863.

52. V. Malandraki, and D. Toll, "Triaxial Tests on Weakly Bonded Soil With Changes in Stress Path," *Journal of Geotechnical and Geoenvironmental Engineering* 127, no. 3 (2001): 282–291, https://doi.org/10.1061/(ASCE)1090-0241(2001)127:3(282.

53. F. Sariosseiri, and B. Muhunthan, "Effect of Cement Treatment on Geotechnical Properties of Some Washington State Soils," *Engineering Geology* 104, no. 1 (2009): 119–125, https://doi.org/10.1016/j.enggeo.2008.09.003.

54. ASTM D2216-17, *Standard Test Method for Laboratory Determination of Water (Moisture) Content of Soil and Rock by Mass* (ASTM, 2017).

55. ASTM D854-23, *Standard Test Methods for Specific Gravity of Soil Solids by Water Displacement Method* (ASTM, 2023).

56. ASTM D4318-17, *Standard Test Methods for Liquid Limit, Plastic Limit, and Plasticity Index of Soils* (ASTM, 2018).

57. ASTM D6913-04, *Standard Test Methods for Particle Size Distribution (Gradation) of Soils Using Sieve Analysis* (ASTM, 2009).

58. ASTM C618-08, *Standard Specification for Coal Fly Ash and Raw or Calcined Natural Pozzolan for Use in Concrete* (Annual Book of ASTM Standards, 2008).

59. ASTM D698-12, *Standard Test Methods for Laboratory Compaction Characteristics of Soil Using Standard Effort* 3 (2012): (ASTM International, 2012).

60. DCCMS-03, *Department of Climate Change and Meteorological Services* (DCCMS, 2025).

61. ASTM D3080, *Standard Test Method for Direct Shear Test of Soils Under Consolidated Drained Conditions* (ASTM International, 2011).

62. ASTM D7181, *Standard Test Method for Consolidated Drained Triaxial Shear Test of Soils* (ASTM, 2020).

63. U. Calik, and E. Sadoglu, "Classification, Shear Strength, and Durability of Expansive Clayey Soil Stabilized With Lime and Perlite," *Natural Hazards* 71, no. 3 (2014): 1289–1303, https://doi.org/10.1007/s11069-013-0950-1.

64. T. Nagaraj, and N. Miura, *Soft Clay Behaviour Analysis and Assessment* (CRC Press, 2021).

65. X. Kang, L. Ge, and W. C. Liao, "Cement Hydration-Based Micromechanics Modeling of the Time-Dependent Small-Strain Stiffness of Fly Ash-Stabilized Soils," *International Journal of Geomechanics* 16, no. 3 (2016), https://doi.org/10.1061/(ASCE)GM.1943-5622.0000552.

66. S. Pu, Z. Zhu, W. Song, et al., "Mechanical and Microscopic Properties of Cement Stabilized Silt," *KSCE Journal of Civil Engineering* 24 (2020): 2333–2344, https://doi.org/10.1007/s12205-020-1671-0.

67. W. Lee, M. J. Lee, and S. K. Choi, "Shear Strength of Artificially Cemented Sands," *Marine Georesources and Geotechnology* 27 (2009): 201–216, https://doi.org/10.1080/10641190902967051.

68. H. B. Lyu, J. X. Gu, J. R. Zhou, and B. Li, "Mechanical Behavior and Particle Breakage of Calcareous Sand in Triaxial Test," *Marine Geophysical Research* 44 (2023), https://doi.org/10.1007/s11001-023-09525-0.

69. A. S. Azneb, S. Banerjee, and R. G. Robinson, "Shear Strength of Cement-Treated Marine Clay Under Triaxial and Plane Strain Conditions," *Proceedings of the Institution of Civil Engineers-Ground Improvement* 3 (2021): 143–156, https://doi.org/10.1680/jgrim.18.00090.

70. M. Feng, S. Liu, J. Wang, and Y. Hu, "Influence of Stabilisers on the Unconfined Compressive Strength of a Fine Soil," *Geotechnical Research* 7, no. 4 (2020): 209–217, https://doi.org/10.1680/jgere.20.00030.

71. ISO 14040, *Environmental Management—Life Cycle Assessment—Principles and Framework* (International Organisation for Standardisation, 2006).

72. I. Faridmehr, M. L. Nehdi, M. Nikoo, G. F. Huseien, and T. Ozbakkaloglu, "Life-Cycle Assessment of Alkali-Activated Materials Incorporating Industrial Byproducts," *Materials* 14, no. 9 (2021): 2401, https://doi.org/10.3390/ma14092401.

73. C. Kulasuriya, V. Vimonsatit, and W. P. S. Dias, "Performance Based Energy, Ecological and Financial Costs of a Sustainable Alternative Cement," *Journal of Cleaner Production* 287 (2021): 125035, https://doi.org/10.1016/j.jclepro.2020.125035.

74. J. Yu, H. L. Wu, D. K. Mishra, G. Li, and C. K. Y. Leung, "Compressive Strength and Environmental Impact of Sustainable Blended Cement With High-Dosage Limestone and Calcined Clay (LC2)," *Journal of Cleaner Production* 278 (2021): 123616, https://doi.org/10.1016/j.jclepro.2020.123616.

75. A. F. Zidan, "Strength and Consolidation Characteristics for Cement Stabilized Cohesive Soil Considering Consistency Index," *Geotechnical Geological Engineering* 38, no. 5 (2020): 5341–5353, https://doi.org/10.1007/s10706-020-01367-6.